International Journal of Applied Pharmaceutics

ISSN- 0975-7058 Vol 15, Issue 1, 2023

Original Article

ENHANCED AQUEOUS SOLUBILITY AND *IN VITRO* DISSOLUTION OF THE ANTI-HYPERLIPIDEMIC AGENT USING SYNTHESIZED SOLID DISPERSION CARRIER

DARSHAN R. TELANGE, SURENDRA S. AGRAWAL, ANIL M. PETHE, ANKITA V. HADKE*

Datta Meghe College of Pharmacy, Datta Meghe Institute of Higher Education and Research (Deemed to be University), Sawangi (Meghe) Wardha. 442001, Maharashtra, India.
***Email: ankita.pharmacy@dmimsu.edu.in**

Received: 23 Aug 2022, Revised and Accepted: 30 Nov 2022

ABSTRACT

Objective: To improve ATN's solubility, permeability, and dissolution rate of pentaerythritol-eudragit®RS100 co-processed excipients (CE) and their potential as a solid dispersion carrier (ATN-CE-SD).

Methods: The ATN-CE-SD was prepared using the solvent evaporation technique. The pure ATN, physical mixture, CE carrier, and optimized ATN-CE-SD was physicochemically characterized using Scanning electron microscopy, Fourier transforms infrared spectroscopy, differential scanning calorimetry, powder x-ray diffractometry, solubility, and *in vitro* dissolution was used to evaluate solid dispersions.

Results: Physical and chemical analysis showed that ATN-CE-SD formed via the involvement of weak intermolecular forces of attraction between CE carrier and ATN. The prepared solid dispersion showed the drug content around ~ 96.94 % w/w, indicating that the solvent evaporation method improved the encapsulation of ATN and, thus, enhanced its drug content. Compared to pure ATN (~ 0.11 mg/ml), ATN-CE-SD (1:2) significantly increased the aqueous solubility by around ~ 25-fold (~ 2.78 mg/ml), indicating solid dispersion improves the solubility of ATN. ATN-CE-SD enhanced the rate of dissolution of ATV (~ 65 %) compared to pure ATN (~ 25 %) and PM (~ 34 %). Likewise, ATN-CE-SD (1:2) improved the rate and extent of ATN (~ 60 %) across the biological membrane compared to pure ATN (~ 22 %) and PM (~ 32 %). The ATN-CE-SD (1:2) improved the dissolution efficiency by around ~ (57.31%) compared to pure ATN (~ 7.02%) and PM (~ 20.43%). According to the study, co-processed excipients could serve as a promising solid dispersion carrier and improve ATN's water solubility, permeability, and dissolution rate.

Conclusion: Based on the results, it is possible to use synthetic solid dispersion carriers as alternatives to improve the low water solubility and permeability of ATN.

Keywords: Atorvastatin, Co-processed excipients, Eudragit®RS100, Pentaerythritol, Solid dispersion

DOI: https://dx.doi.org/10.22159/ijap.2023v15i1.46657. Journal homepage: https://innovareacademics.in/journals/index.php/ijap

INTRODUCTION

Atorvastatin (ATN) is a well-known HMG-CoA reductase enzyme inhibitor and cholesterol-lowering medication. ATN reduces cholesterol production by blocking the formation of mevalonate from HMG-CoA [1]. ATN has a limited oral bioavailability of only 12%, probably due to its poor water solubility of 0.1 mg/ml, severe first-pass metabolism, crystalline behaviour, and short half-life of 1–2 h. ATN was placed in Biopharmaceutical Classification System (BCS) class II due to its poor water solubility and high intestinal permeability profile. In addition, ATN's poor solubility in aqueous solution and shorter half-life result in more frequent dosages, which can have significant adverse effects such as arthralgia, rhabdomyolysis, abnormalities in the liver and renal failure [2]. We suggest a suitable carrier to improve ATN's low water solubility, permeability, and biopharmaceutical properties.

Numerous formulation strategies that could improve ATN's solubility, permeability, and dissolution rate have been described by the authors. Tablets [3], nano solid dispersion [4], semi-solid binary system [5], nanocrystals [6], binary and ternary solid dispersion [7], and solid dispersion [1] are some of these methods. A comprehensive analysis of various formulation systems revealed several flaws, along with a minor improvement in the biopharmaceutical characteristics of ATN. As an illustration, neem gum-based solid ATN dispersion increased its restricted aqueous solubility by ~ 3 and 4 times compared to pure ATN [1]. We developed the co-processed excipients as solid dispersion carriers with higher water solubility, permeability, and dissolving rate of ATN in response to the identified inadequacies and ineffectiveness of the existing formulations.

To create a single composite excipient with better functionality than a physical mixture of the same excipients, two or more existing excipients are combined at the sub-particle level to create co-processed excipients [8]. It offers enhanced compressibility, dilution potential, disintegration property, flow qualities, and decreased lubrication sensitivity. Additionally, it improved the solubility, wettability, stability, and gelling qualities of excipients, active pharmaceutical ingredients (API), and food additives [9]. Using co-processed excipients as solid dispersion carriers to improve the biopharmaceutical properties of BCS class II medications has drawn increased attention from scientists due to these advantages. By reducing drug particle size to sub-micron particles, switching the drug's crystalline state to a high energy amorphous state, and improving the drug's wettability. The solid dispersion formulation significantly improved the solubility, permeability, dissolution, and pharmacokinetic profile of poorly aqueous soluble drugs [10-12]. Co-processed excipients have been used in prior studies to demonstrate the use of glimepiride, a BCS class II medication, as a solid dispersion carrier with an accelerated dissolution rate [13]. In this study, we investigated whether pentaerythritol-Eudragit®RS100 co-processed excipients (CE) might be used as a solid dispersion carrier to improve the solubility, permeability, and dissolution rate of ATN. The crystalline ATN particles are converted into a high-energy state amorphous powder using the CE carrier and solvent evaporation process, which increases the drug surface area and speeds up solubility. Pentaerythritol offers maximum encapsulation and accommodation to all crystalline molecules due to its structural similarity and low lattice energy. By dispersing the drug and partially or entirely amorphizing it, this solid dispersion formation mechanism increases the drug's solubility and rate of dissolution [14]. A polymer called Eudragit®RS100 (ERS) is a cationic copolymer (ethyl acrylate, methyl-methacrylate, chlorotrimethylammonioethyl methacrylate). A regulated, extended, and localized drug administration to physiological media is made possible by the presence of 4.5–6.8% functional quaternary ammonium groups (FQAG) on the ERS polymer. This interaction helps to encapsulate the drug and form the drug-ERS complex [15].

Pentaerythritol and ERS can deliver medicines. However, their combined utilization and the clinical uses of PECE as a solid dispersion carrier have not been thoroughly investigated. Pentaerythritol and ERS have only been mentioned in a few papers by the study teams of Chiou *et al.* and Barzegar-Jalali *et al.* [16, 17]. These studies found that formulations lacked thorough and organized Physico-chemical and functional characterization. The PECE carrier was constructed, and its viability as a solid dispersion carrier was therefore investigated in the current work. The quaternary ammonium groups (QAG) of ERS polymer interacted chemically (i.e., by ion-pair and hydrogen bonding) with the hydroxyl groups of pentaerythritol in the presence of ethanol to produce the CE carrier. This interaction makes it even easier for the amorphous ERS polymer to fit into the pentaerythritol crystal lattice. Pentaerythritol has strong dominance in the CE carrier, as demonstrated by FT-IR, DSC, and PXRD studies. In formulations for solid dispersions, the COOH, N-H, and O-H groups of ATN could produce strong electrostatic interactions with the CE carrier's QAG and hydroxyl groups. It makes it possible for highly ordered, crystalline ATN to fit within the pentaerythritol crystal lattice, resulting in complete amorphization and the development of molecular dispersion with increased ATN solubility and dissolving rate.

This research, intended to serve as "proof of concept," examines the viability of using CE as a solid dispersion carrier to increase ATN's solubility, permeability, and dissolution rate. Two steps were taken to complete this task. First, the solvent evaporation method was used to create the CE carrier, and then the same technique was used to develop the CE-based solid dispersion of ATN. The optimized formulations were examined using Fourier transforms infrared spectrophotometry, scanning electron microscopy, differential scanning calorimetry, solubility analysis, and *in vitro* dissolution tests.

MATERIALS AND METHODS

Materials

High-grade (>99%) atorvastatin calcium was purchased from Alkem Laboratories Ltd. in Mumbai, India. We bought pentaerythritol from Sigma-Aldrich Corporation in St. Louis, Missouri, USA. From Bangalore, India's Chemsworth Pvt. Ltd., Eudragit®RS100 was purchased. Other analytical grade chemicals were bought from Loba Chemicals Pvt. Ltd., Mumbai, India.

Preparation of pentaerythritol-eudragit®RS100 co-processed excipient (CE)

The pentaerythritol-eudragit®RS100 co-processed excipients (CE) carrier was created using a slightly modified method from one literature published in Elsevier [13, 18]. Briefly, 50 ml of ethanol was used to dissolve ~ 100 mg of pentaerythritol and ~100 mg of eudragit®RS100 (ERS). The mixture of components in ethanol was well mixed to achieve homogeneity. For 15 min, the homogeneous solution was heated in a water bath at 80 °C. A hot solution was poured into the china dish to create CE powder and set aside for the night. The CE powder was dried in a hot air oven for two hours at 60 °C. Dried CE powder was ground and stored in amber-colored glass vials with nitrogen purged until further physico-chemical evaluation.

Preparation of atorvastatin-CE solid dispersion (ATN-CE-SD)

Our group previously described solvent evaporation process was used to manufacture the CE carrier-based solid dispersion of atorvastatin (ATN-CE-SD) with a few minor modifications [19]. The ~ 40 mg of ATN and ~ 80 mg of CE carrier were precisely weighed following the stoichiometric ratio (1:2) before being added to a previously cleaned mortar and pestle. A magnetic stirrer created a thick paste by stirring the other ingredients with 10 ml of absolute ethanol. It was continuously triturated until the ethanol evaporated, creating the ATN-CE-SD dry porous solid mass. The solid mass was gathered and dried in the oven for 24 h at 40 °C. Vacuum drying at 40 °C for 24 h after sieving (#60 mesh sizes) dried solid dispersion powder. A nitrogen-purged amber-colored (light-resistant) glass vial was used to transfer the dried ATN-CE-SD powder, which was then kept in a desiccator until further testing.

Scanning electron microscopy (SEM)

An electron microscope is used to examine the surface morphology, content, and placement of the materials within the formulations. Pure ATN, CE carrier surface texture, and optimized ATN-CE-SD (1:2) formulations were examined using a scanning electron microscope (Model: Supra®55, Carl Zeiss NTS Ltd., Germany). The analysis was conducted following the method described earlier [20]. Briefly, a thin layer (film) of the weighed samples (~ 50 mg) was applied on double-faced carbon tape. The sample was coated with gold and scanned at a 10 kV accelerating voltage using the sputter coating method. The software attached to the equipment, known as Smart SEM® V05.06, was used to read and analyze the scanned pictures.

Fourier transforms infrared spectroscopy (FT-IR)

Using a Fourier transform infrared spectrophotometer, the samples of pure ATN, pentaerythritol, ERS, PM (1:2), CE carrier, and improved ATN-CE-SD (1:2) formulations were examined (Model: FTIR-8300, Shimadzu, Kyoto, Japan). Briefly, agate mortar and pestle were used to make the powder mixture of the sample and potassium bromide (KBr, FT-IR grade), which was then crushed into thin clear discs using a Mini Hand Press Machine (Model: MHP-1, P/N-200-66747-91, Shimadzu, Kyoto, Japan). The scan range for the sample discs was between 4000 and 400 cm-1. FT-IR-connected software reads and interprets the scanned images (Control Software, Version 1.10). For sample FT-IR analysis, the process developed earlier was followed [21].

Differential scanning calorimetry (DSC)

According to a method previously described [22], the thermal properties of the formulation components of pure ATN, pentaerythritol, PM (1:2), CE carrier, and optimized ATN-CE-SD (1:2) formulations were investigated. The differential scanning calorimeter was a DSC-1821e from Mettler Toledo AG, Analytical, Schwerzenbach, Switzerland. Briefly, the weighed samples of 2 mg were sealed in the instrument's aluminium pan. Within a temperature range of 0 to 400 °C, the sealed samples were heated at a rate of 10 °C/min. After heating, the software with the equipment was used to read, interpret, and analyze the DSC curves (UA, V4.5A, build 4.5.0.5).

Powder x-ray diffractometry (PXRD)

In this investigation, samples of pure ATN, pentaerythritol, PM3 (1:4), PECE carrier, and ATN-CE-SD (1:2) formulations were analyzed using PXRD equipment (Model: D8 ADVANCE, Bruker AXS, Inc., Madison, WI, USA). The samples~ 50 mg were quickly placed into the section used for sample analysis. CuKβ radiation was used to irradiate the samples. A silicon strip-based detector was used to find the signal of radioactively contaminated materials (LYNXEYE™). The produced diffraction pattern of each sample was read and examined. The method reported earlier was followed in this study [23].

Estimation of drug content

The ATN content in the prepared ATN-CE-SD formulations was calculated using a technique previously described by Dhore *et al.* [24]. Shortly after being weighed, the ATN-CE-SD formulations equivalents to around ~ 40 mg of ATN were put into a 100 ml volumetric flask. The weighed powder was combined with newly made 100 ml of phosphate buffer (0.05 M, pH 6.8) using a magnetic stirrer. The dissolved materials were recovered after membrane filtration (0.45). Using a UV-visible spectrophotometer, a tiny amount of the filtrate was diluted and tested for absorbance at the detection wavelength of about 246 nm (Model: V-630, JASCO International Co., Ltd., Tokyo, Japan). A different carrier solution was made using the same procedure as the formulations and compared to the sample solution to avoid carrier interference. The ATN content in the ATN-CE-SD formulations was calculated using the equation explained below.

$$\text{ATN content (\%)} = \frac{\text{Total ATN (mg)} - \text{free ATN (mg)}}{\text{Total ATN (mg)}} \times 100$$

Saturation solubility analysis

Pure ATN, PM, and ATN-CE-SD formulations underwent an aqueous solubility investigation [24]. Briefly, samples of pure ATN, PM, and ATN-CE-SD formulations were weighed and put into 10 ml glass vials with screw caps. 10 ml of distilled water was added to the weighed samples, which were well combined. A rotary shaker (Model: RS-24 BL, REMI Laboratory Instruments, Remi House, Mumbai, India) was used to stir the vial contents for 24 h at 37 °C. A membrane filter (0.45) was used to filter the agitated solution, and the filtrate was collected. Using a UV-visible spectrophotometer, an aliquot of the filtrate was diluted and tested for ATN absorbance at a maximum wavelength of around 239 nm (Model: V-630, JASCO International Co., Ltd., Tokyo, Japan). The sample solution and the blank were put to the test. The analysis was carried out in a warm environment.

***In vitro* dissolution studies**

The USP type II paddle dissolution test apparatus was used to compare the *in vitro* dissolution profiles of pure ATN and optimized ATN-CE-SD (1:2) formulations in phosphate buffer (0.05 M, pH 6.8). (Model: TDT-08LX, Elecctrolab India Pvt. Ltd., Mumbai, India). The dissolution investigations were conducted following past literature that had been published [25]. The samples of PM (1:2) ~ 40 mg of ATN, pure ATN ~ 40 mg, or improved ATN-CE-SD (1:2) formulations ~ 40 mg of ATN were weighed and mixed into 900 ml of dissolution media in the dissolution flask. At a speed of 100 RPM, the scattered samples were swirled. The dissolving medium's temperature was maintained at 37±0.5 °C for two hours. After stirring, a small aliquot of the sample was taken and diluted appropriately, and its ATN absorbance was measured against a blank solution using a UV-visible spectrophotometer (Model: V-630, JASCO International Co., Ltd., Tokyo, Japan). The condition of the sink was kept throughout the analysis. The % cumulative ATN release was used to compute and report the absorbance values for formulations with pure ATN and ATN-CE-SD (1:2).

Dissolution efficiency

Drug and formulation dissolving characteristics are described using dissolution efficiency [31]. The equation was used to determine the dissolving efficiency of pure ATN and improved ATN-CE-SD (1:2) formulations in phosphate buffer dissolution media (2).

$$DE = 1 + \frac{\int_{t1}^{t2} y.\,dt}{y100 \times (t2 - t1)} \times 100$$

In the equation above, term y represents the percentage of ATN dissolved in phosphate buffer, whereas term DE represents the area under the curve (AUC) of the dissolution curve between times points. It is expressed as a percentage of the maximal dissolution of y100 for the same time frame. Additionally, the numerator portion of the DE was approximated using the previously described equation.

$$AUC = \sum_{i=1}^{i=n} - \frac{(t1 - ti - 1)(Yi - 1 + Yi)}{2}$$

In this equation, the ti represents the ith time point, and Yi represents the percentage of ATN dissolved at time ti. Further estimation of pure ATNs and improved ATN-CE-SD (1:2) formulations were done using the created DDSolver® tool.

Everted rat intestine-based permeation studies

Using a specifically created everted rat intestine apparatus described earlier in the literature, the comparative permeation performance of pure ATN, PM (1:2), or optimized ATN-CE-SD (1:2) formulations across the everted rat intestinal membrane was examined. The Dhore *et al.* [24] approach was used throughout the entire study, including the creation of permeation media and everted rat intestinal membrane. In a nutshell, the cleaned and mended everted rat intestinal membrane was placed between the two tapered ends of the device. Kreb's solution was newly made and poured into the apparatus. A 250 ml beaker holding testing solutions of pure ATN at ~ 100 mg/ml, PM at ~ 100 mg/ml, or optimized ATN-CE-SD at 100 mg/ml made in Kreb's solution was used to submerge the solution-filled device. The permeation medium's temperature was constant at 37±0.5 °C for two hours while agitated at 25 RPM. The medium was mixed while aerated with a combination of 95% O2 and 5% CO2. The small aliquot was then taken at the predetermined interval, filtered, diluted, and its absorbance at a maximum wavelength of 241 nm was measured against the blank solution using a UV-visible spectrophotometer (Model: V-630, JASCO International Co., Ltd., Tokyo, Japan). The cumulative% of ATN penetrated was computed and given as the comparative absorbance readings of pure medications or formulations.

Statistical analysis

To compare the variations between the test samples, the statistical analysis was done using Dunnett's or student's t-test. The data is displayed as mean±standard deviation. A p-value of *0.05* or less was regarded as statistically significant.

RESULTS AND DISCUSSION

Preparation of CE and ATN-CE-SD

Pentaerythritol and ERS were combined through the evaporation of an ethanol-based solvent to produce the CE carrier. The ERS containing 5% functional quaternary ammonium may have resulted from ethanol-induced chemical reactions involving pentaerythritol hydroxyl groups. This interaction makes it easier for amorphous ERS to fit into the pentaerythritol crystal lattice structure, which leads to creating a CE carrier with high pentaerythritol dominance in the FT-IR, DSC and PXRD spectrum.

ATN, a lipid-lowering drug, exhibits more excellent solubility in organic solvents than in aqueous solutions [27]. Utilizing the solvent evaporation process, this Physico-chemical characteristic of ATN is used further to prepare its solid dispersion. According to earlier investigations, ATN solid dispersion was developed using water [1] and methanol [28] as the preferred solvents. Utilizing a CE carrier, we created an ATN solid dispersion using these solvents. The ATN and CE demonstrate reduced solubility and water dissolution during preparation, indicating the precipitation of formulation ingredients. The CE carrier revealed low solubility and dissolution in methanol, whereas the ATN exhibited good solubility. It resulted in the formulations failing due to the carrier precipitation. To solve the solubility and dissolution issue, the authors investigated various solvents, such as acetone, 1,4 dioxane, and pure ethanol. The ATN and CE carrier had the same solubility problems in acetone and 1,4-dioxane as in water and methanol. In addition to the problem with solubility, the 1,4-dioxane solvent's documented toxicity profile in humans limits its usage in the manufacture of solid dispersion. Finally, the 100% ethanol formed an amorphous ATN-CE-SD with fair solubility and dissolution for the ATN and CE carriers. It implies that the solubility and dissolution of the ingredients, leading to the formation of an amorphous ATN solid dispersion, may be improved by the hydrogen bonds between the ethanol, ATN, and CE carrier.

SEM

Fig. 1 shows the SEM images of pure ATN, CE carrier formulations, and ATN-CE-SD (1:2) (A, B and C). Pure ATN SEM images are displayed in (fig. 1A). Its particles had an ill-defined morphology and appeared as clusters of small and big needle-shaped particles. According to the SEM images of the CE carrier (fig. 1B), the interaction between pentaerythritol and ERS in the presence of ethanol could result in the formation of a rough and porous surface CE carrier. In contrast, SEM images of ATN-CE-SD (1:2) (fig. 1C) formulations seem porous with irregular shape and surface features, indicating that ATN needle-shaped particles were entrapped within the porous surface of the CE carrier. It implies that the triturated-assisted decreased ATN particles can become trapped inside the carrier's porosity region, resulting in considerable particle interaction and the formation of amorphous solid dispersion formulations. Additionally, the solvent evaporation technique may help form amorphous solid dispersion.

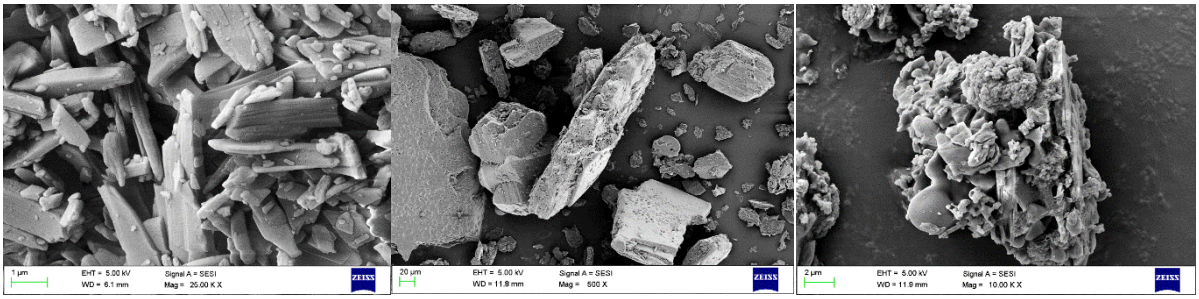

Fig. 1: Scanning electron micrographs of (A) ATN, (B) CE carrier,(C) optimized ATN-CE-SD (1:2) formulation

FT-IR

Fig. 2 (A to D) shows the FT-IR spectrum of various formulations, including pure ATN, PM (1:2), CE carrier, and optimized ATN-CE-SD (1:2). The free hydroxyl and bonded group (O-H stretching) absorption peaks in the pure ATN's FT-IR spectra (fig. 2A) are at 3675.2 and 3213.0 cm-1, 3362.1 cm-1 for the amide (N-H stretching), and 2970.7 cm-1 for the aromatic group, respectively (C-H stretching). Additionally, it displays peaks for pyrrole at 1315.8 cm-1, amide at 1580.4 cm-1, and keto-amide at 1649.2 cm-1 (C=O stretching) (C-N stretching). These peaks closely match the previously published ATN [29, 30]. The additive peaks in the FT-IR spectra of PM (1:2) (fig. 2B) are pentaerythritol, ERS, and pure ATN. The pentaerythritol peaks were dominant in the FT-IR spectra of the CE carrier (fig. 2C), with the allowance of a low-intensity ERS peak at 1722.0 cm-1 for C=O stretching. This peak in the CE spectrum suggests that the ERS reacted with pentaerythritol at the level of the carbonyl group. Finally, the ATN-CE-SD (1:2) (fig. 2D) shows a spectrum with the occurrence of new and retention of old peaks identical to pentaerythritol and the CE carrier. The fact that the low-intensity peak at 3302.4 cm-1 was replaced by a high-intensity new peak at 3309.9 cm-1 suggests that pentaerythritol O-H groups significantly interacted with the O-H and N-H groups of ATN and ERS via intermolecular forces of interaction (i.e., hydrogen bonding, ion-dipole, and van der Waals forces) may have caused the merging of these Additionally, the spectrum exhibits the retention of ATN and ERS peaks in the lower frequency range, proving that ATN, polymer, and carrier do not interact. Based on a comparison of the spectra, it appears that the interaction forces between the O-H and N-H groups of the ATN, polymer, and CE carrier primarily cause solid dispersion.

DSC

The pure ATN, CE carrier, and ATN-CE-SD (1:2) thermograms are displayed in (fig. 3A, 3B and 3C). Two tiny endothermic peaks can be seen on the pure ATN thermogram (fig. 3A). Dehydration is most likely to blame for the first peak, recorded at around 132.7 °C, and melting point for the second peak, which was recorded at about 158.43 °C [28]. The CE carrier (fig. 3B) exhibits a thermogram comparable to that of pentaerythritol with shifting peak position and intensity, showing strong interaction between them. It is suggested that pentaerythritol low lattice energy accommodates and wraps ERS particles, allowing their dispersion and merging of peaks to produce the CE carrier with pentaerythritol thermogram dominance [16, 31]. The thermograms of ATN-CE-SD (1:2) were shown in (fig. 3C) and had two distinct properties. The thermograms exhibit similarities to pentaerythritol with two different peak positions and intensities of approximately 198.2 °C and 269.22 °C, respectively. First, there are no ATN peaks at all. These traits show that the CE carrier has an advantageous association with ATN and has produced an amorphized solid dispersion. According to this association, pentaerythritol phase transition behaviour, which was observed around ~ 23 Cal/degree/mole dominance, may accommodate crystalline ATN particles within its crystal lattice, facilitating their dispersion, amorphization and subsequent formation of amorphous solid dispersion [16]. These thermal changes confirm the creation of solid dispersion compared to the initial peaks.

PXRD

The diffractograms of the pure ATN, CE carrier, and ATN-CE-SD (1:2) formulations are shown in fig. 4 (A, B and C). The sharp and intense diffraction peaks on the 2θ scale are visible in pure ATN (fig. 4A) at positions 11° (~ 1250 Lin counts), 20° (~ 600), 22° (~1150), 23° (~ 600), and 24° (~ 600), respectively. Additionally, ATN showed broad and diffuse peaks at 3°, 6°, 9°, 10°, 12°, and 25°, which supported earlier published research [32] and indicated ATN crystalline composition. The diffraction peaks of the CE carrier are shown in (fig. 4B). It showed the same peak characteristics as the original pentaerythritol diffraction pattern. Several little diffused peaks were also seen between the range of ~ 400 and 600, suggesting that ERS polymer aids in forming CE carriers. The creation of the pentaerythritol peaks in the CE carrier shows that pentaerythritol may enclose the ERS within its crystal lattice structure, causing dispersion, amorphization, and merging of the ERS peaks into the CE carrier peaks.

In contrast to the original ATN and CE carrier peaks, the ATN-CE-SD (1:2) formulations (fig. 4C) showed the absence of ATN crystalline peaks and the appearance of low-intensity pentaerythritol peaks, indicating that the CE carrier successfully interacted with ATN in the presence of ethanol and produced amorphized solid dispersion. According to this process, the CE multifunctional carrier with pentaerythritol predominance may fit the complete crystalline ATN particle within its crystal lattice because of its structural resemblance to the API. This interaction results in ATN-CE-SD formulations with excellent surface area properties and complete ATN dispersion and crystalline amorphization. The CE carrier successfully reduced its crystalline condition by encapsulating the ATN and created the ATN-CE-SD formulations, according to this characterization.

Estimation of drug content

The ATN content in the ATN-CE-SD (1:2) solid dispersions based on the CE carrier was around ~ 96.94% w/w, demonstrating improved interaction and association between ATN and the CE carrier. Formulations with drug concentrations more than>90% w/w indicate that the CE carrier could improve ATN dispersion, interaction, and subsequent assimilation within the carrier matrix, boosting the ATN content in the CE-based solid dispersion.

Saturation solubility studies

The pure ATN exhibits low aqueous solubility of ~ 0.11 mg/ml, which indicates that it belongs to the BCS II class [2]. The modest increase in aqueous solubility of ATN by the PM-containing CE carrier, which was around ~ 0.27 mg/ml, may be attributed to the close association and subsequent interaction of the highly aqueous soluble CE carrier with the ATN particles, which led to partial amorphization of the ATN particles and improved their aqueous solubility. The adjusted ATN-CE-SD (1:2) formulations increased the solubility of the ATN by around ~ 2.78 mg/ml in water by almost ~ 25 times, proving that the carrier increased solubility. This result shows that the promising pentaerythritol appearance in the thermal and PXRD spectra is a component of the CE carrier. The whole ATN particle population can fit inside its crystal lattice due to its structural similarity and low lattice energy, which may allow for the establishment of weak interparticle forces. This interaction results in the amorphous ATN-CE-SD formulation with strong solubility properties and aids the dispersion and decrease of ATN crystallinity [33, 34]. Additionally, it implies that the amorphization and solvation effects of amorphous ERS on ATN particles may increase their water solubility [17].

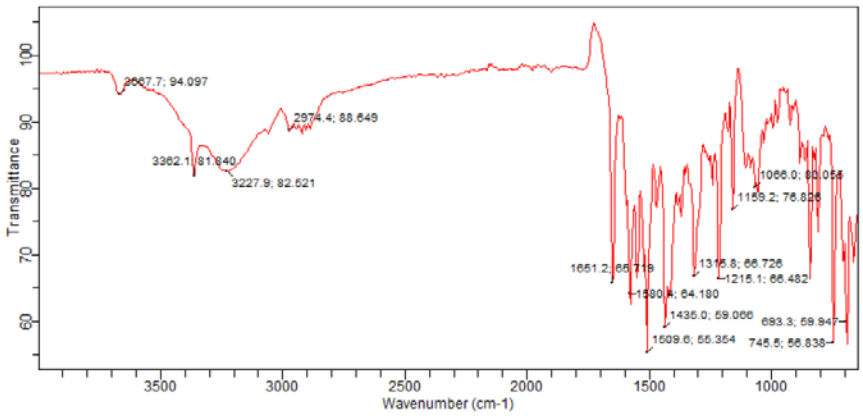

A)

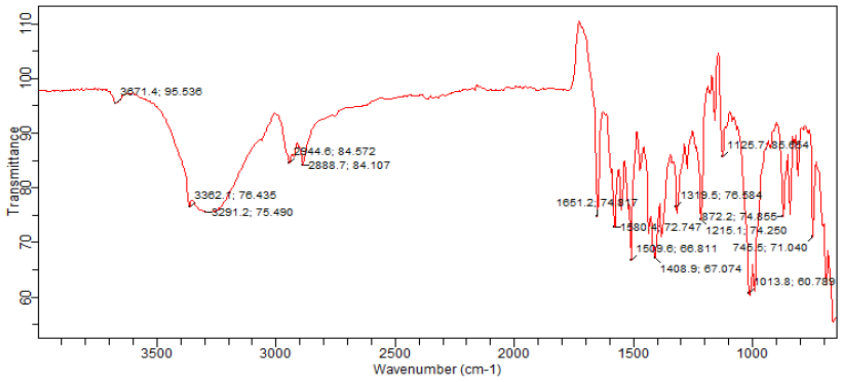

B)

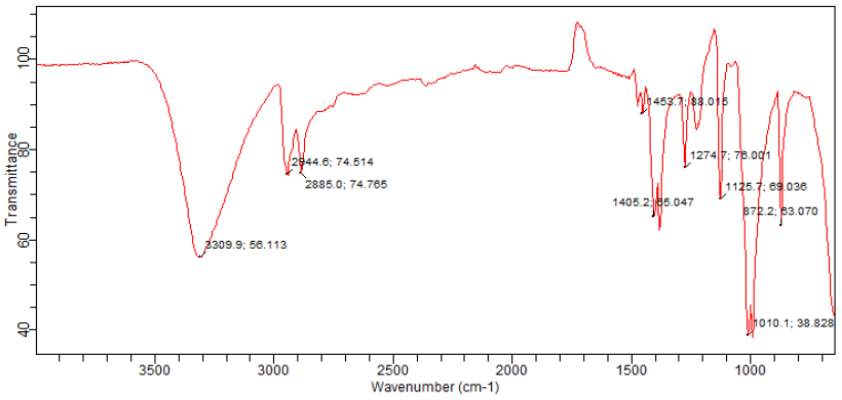

C)

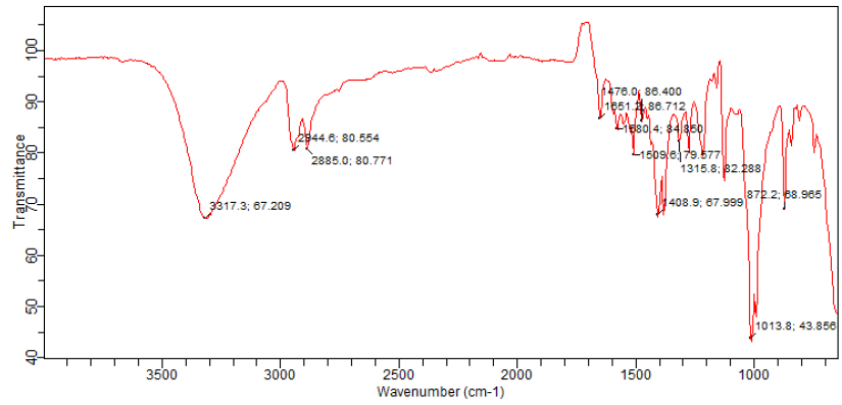

D)

Fig. 2: Fourier transforms infrared spectra of (A) pure ATN, (B) PM (1:2), (C) CE carrier, (D) optimized ATN-CE-SD (1:2) formulations

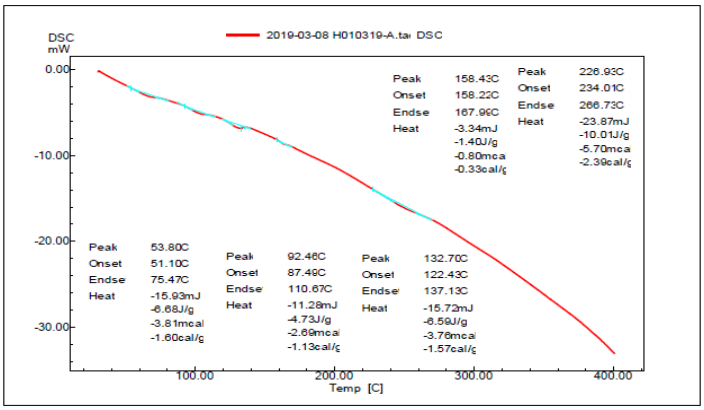

A)

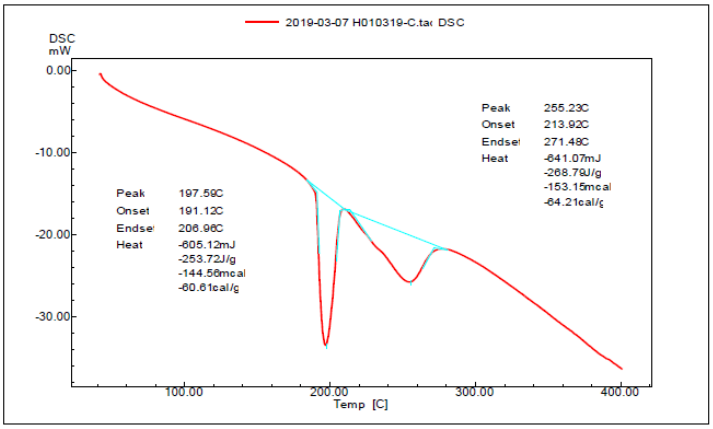

B)

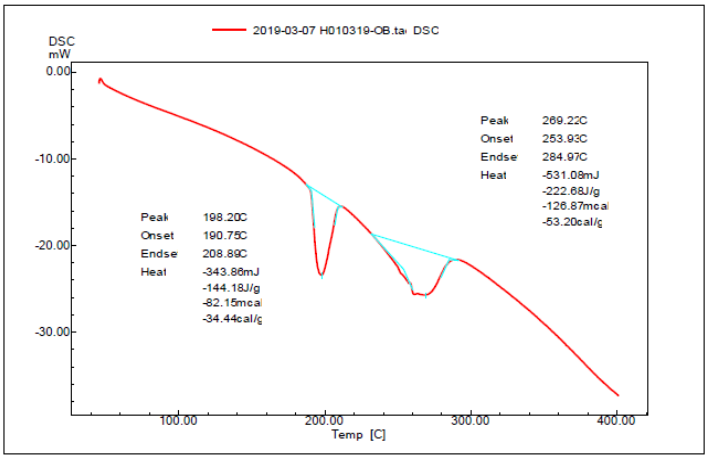

C)

Fig. 3: Differential scanning calorimetry thermograms of A) pure ATN, B) CE carrier C) Optimized ATN-CE-SD (1:2) formulations, Mean value of 3 replications±standard deviation

In vitro dissolution studies

Fig. 5 displays the comparative release performance of ATN from pure ATN, PM (1:2), or optimized ATN-CE-SD (1:2) formulations. The pure ATN showed only ~ 25 % dissolution in phosphate buffer by the end of 120 min, which indicates ATN poor aqueous solubility characteristics match the saturation solubility studies. The PM (1:2) produced a higher ATN dissolution rate than pure ATN. The PM displayed the dissolution pattern in parallel with pure ATN and enhanced the drug dissolution by around ~ 34 % at the end of the period, suggesting that the hydrophilic nature of pentaerythritol and ERS may form a close association with the ATN causing its partial amorphization and thus, enhancing the ATN dissolution. Compared to pure ATN and PM dissolution, the optimized ATN-CE-SD (1:2) significantly improved the ATN dissolution performance. The optimized formulations exhibited ~ 65 % ATN dissolution by the end of 120 min, indicating that the highly soluble CE carrier could improve drug dissolution. This promising result suggests that the combination of solvent evaporation method, synthesized carrier, individual pentaerythritol, ERS, and ethanol solvent could enhance ATN dissolution performance in the dissolution media. The well-established solvent evaporation technique could convert the highly

crystalline ATN particles into high-energy state amorphized particles, facilitating its solubilization and enhancing the dissolution. The hydrophilic CE carrier could develop the association and interaction with ATN's O-H and COOH groups. This association may increase the ATN dispersion within the carrier, improving its dissolution to a great extent. The combined interaction of ERS and pentaerythritol with ATN facilitates the easy accommodation of highly crystalline ATN within the crystal lattice structure of pentaerythritol, causing complete amorphization and formation of molecular dispersion with enhanced ATN dissolution rate. Moreover, the protonation of acidic groups of ATN by the ERS may also find the reason for increasing the drug dissolution rate. Another explanation suggests that the lower amount of ERS in the PECE carrier may diminish the burst effect of ATN and thereby increase its dissolution. Like other hydrophilic carriers, the CE carrier may also inhibit nucleation and crystal growth and prevent the re-precipitation of amorphized API from supersaturated solution, enhancingthe drug dissolution rate. Ethanol semi-polar nature and hydrogen bonding formation capacity could form hydrogen bonding with ATN and carrier, enhancing ATN solubilization and dissolution. Also, the changes in the Physico-chemical attributes of ATN and carriers due to their chemical interaction may improve the ATN dissolution rate.

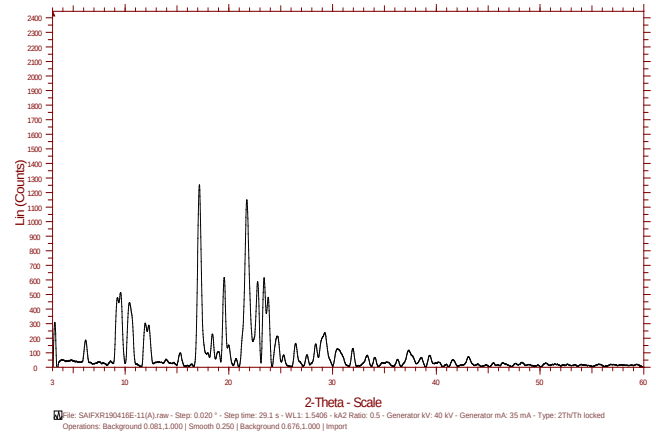

A)

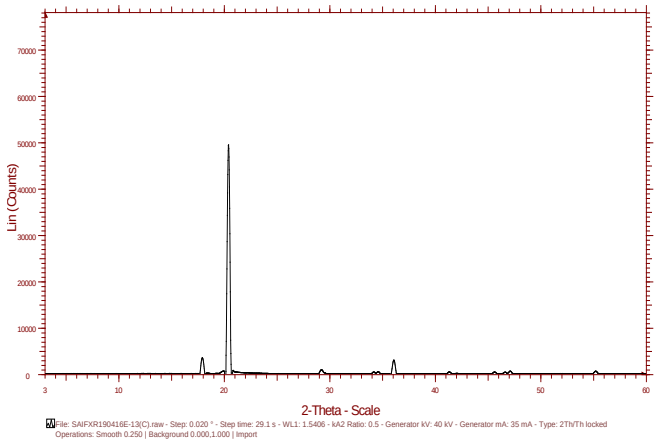

B)

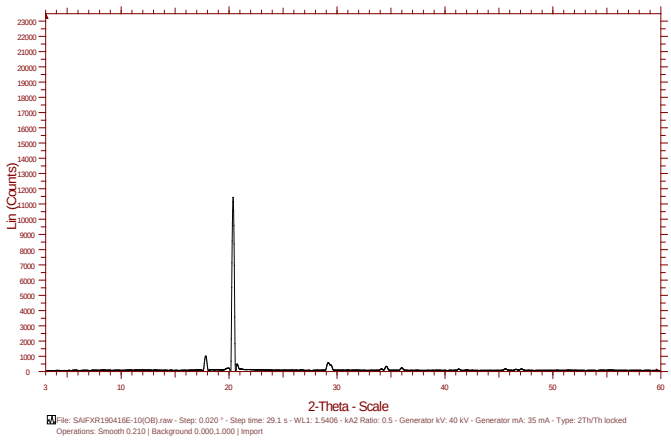

C)

Fig. 4: PXRD spectrum of A) pure ATN, B) CE carrier C) optimized ATN-CE-SD (1:2) formulations, Mean value of 3 replications±standard deviation

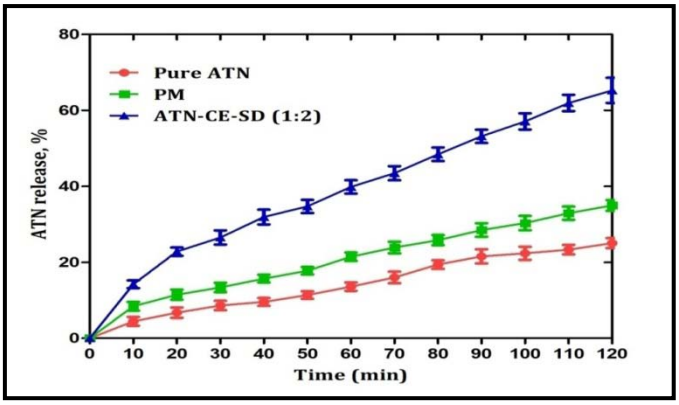

Fig. 5: *In vitro* drug release profiles of ATN from pure ATN, PM (1:2), and optimized ATN-CE-SD (1:2) formulations, Mean value of 3 replications±standard deviation

Dissolution efficiency

The DE value for pure ATN is lowered by ~ 7.02 %. A low DE value of ~ 20.43 % is displayed in the PM (1:2). As opposed to pure ATN and PM, the optimized ATN-CE-SD (1:2) formulations showed higher DE values around ~ 57.31%, demonstrating that optimized formulations improved the DE values. It implies that higher DE values for ATN-CE-SD (1:2) formulations may be due to better solubility of ATN by CE carrier.

Everted rat intestine permeation studies

The comparative permeation profile of pure ATN, PM (1:2), or ATN-CE-SD (1:2) formulations across the everted rat intestine membrane is shown in Fig.6. The pure ATN showed only ~ 22 % ATN permeation across the intestine by the end of the 2-hour testing period indicating its low permeation profile. The PM (1:2) showed a modest improvement in the ATN permeation compared to pure ATN. It demonstrated around ~ 32 % of ATN permeation across the membrane at the end of 120 min. This improvement could attribute to the interaction between the ATN and CE carrier and, subsequently, partial amorphization enhancing the ATN permeation. The ATN-CE-SD (1:2) formulations significantly enhanced the ATN permeation across the biological membrane compared to pure ATN and PM. The ATN-CE-SD (1:2) formulation permeates around ~ 60 % of ATN from the membrane by the end of the permeation period. It indicates that the developed hydrophilic CE carriers may interact with the membrane component and, thus, enhance the ATN permeation. This phenomenon could be explained by the fact that crystal lattice pentaerythritol and ERS could build up the covalent and noncovalent interaction with the amphiphilic components of the membrane. This association may further increase the miscibility of pentaerythritol, ERS or CE carrier within the amphiphilic component of the membrane and, thus, provide easy access to ATN particles across the biological membrane. Moreover, the encapsulation of ATN particles within the highly soluble low lattice energy pentaerythritol may modify the physico-chemical properties of ATN and, thus, improve its permeability.

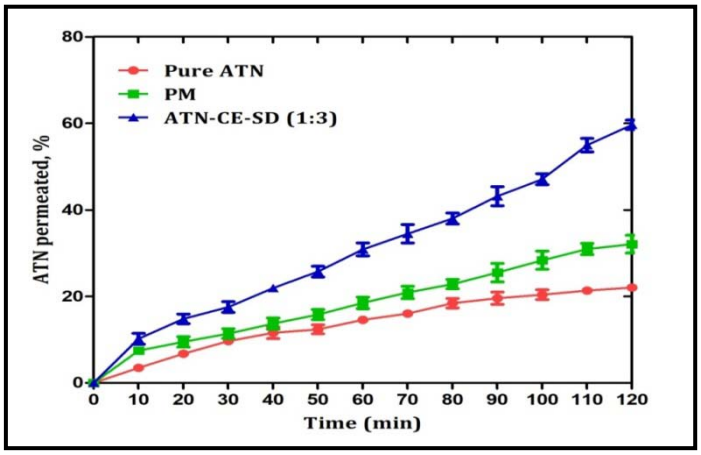

Fig. 6: Ex vivo drug permeation profiles of ATN from pure ATN, PM3 (1:4), and optimized ATN-CE-SD (1:2) formulations, Mean value of 3 replications±standard deviation

CONCLUSION

The CE carrier was effectively synthesized, and its potential as a solid dispersion carrier for improving the low solubility, permeability, and dissolving rate of ATN in water was investigated. The development of CE carriers revealed chemical interactions at work between the hydroxyl groups in pentaerythritol and the quaternary ammonium groups in ERS. The ATN-CE-SD formulations were successfully created using the well-known solvent evaporation process. The physico-chemical analysis validated the synthesis of ATN-CE-SD formulations. According to tests on saturation solubility, when compared to pure ATN and PM, optimal ATN-CE-SD (1:2) formulations increased ATN's aqueous solubility by almost 20 times through accommodation mechanisms, dispersion, and amorphization. The improved ATN-CE-SD (1:2) formulations considerably increased the rate and extent of ATN dissolution compared to pure ATN and PM, according to the *in vitro* dissolution experiments. Ex vivo permeation tests showed that when compared to pure ATN and PM, improved formulations increased the rate and extent of ATN penetration across the biological membrane. Based on the results, it is possible to use synthetic solid dispersion carriers as alternatives to improve the low water solubility and permeability of ATN.

ACKNOWLEDGEMENT

The authors thank Data Meghe College of Pharmacy, DMIMS (DU), Sawangi (Meghe), Wardha for technical support and instrument facilities for completing this research work.

FUNDING

Nil

AUTHORS CONTRIBUTIONS

All the authors contributed equally.

CONFLICT OF INTERESTS

There is no conflict of interest among authors.

REFERENCES

1. Rodde MS, Divase GT, Devkar TB, Tekade AR. Solubility and bioavailability enhancement of poorly aqueous soluble atorvastatin: *in vitro*, ex vivo, and *in vivo* studies. BioMed Res Int. 2014 Jun 14;2014:463895. doi: 10.1155/2014/463895, PMID 24995297.
2. Shete G, Puri V, Kumar L, Bansal AK. Solid state characterization of commercial crystalline and amorphous atorvastatin calcium samples. AAPS PharmSciTech. 2010 Jun;11(2):598-609. doi: 10.1208/s12249-010-9419-7, PMID 20352531.
3. Pusapati RT, Kumar MK, Rapeti SS, Murthy T. Development of co-processed excipients in the design and evaluation of atorvastatin calcium tablets by direct compression method. Int J Pharm Investig. 2014 Apr;4(2):102-6. doi: 10.4103/2230-973X.133059, PMID 25006555.
4. Jahangiri A, Barzegar Jalali M, Javadzadeh Y, Hamishehkar H, Adibkia K. Physicochemical characterization of atorvastatin calcium/ezetimibe amorphous nano-solid dispersions prepared by electrospraying method. Artif Cells Nanomed Biotechnol. 2017 Sep;45(6):1-8. doi: 10.1080/21691401.2016.1202262, PMID 27406894.
5. Shaker MA. Dissolution and bioavailability enhancement of atorvastatin: Gelucire semi-solid binary system. J Drug Deliv Sci Technol. 2018;43:178-84. doi: 10.1016/j.jddst.2017.10.003.
6. Sharma M, Mehta I. Surface stabilized atorvastatin nanocrystals with improved bioavailability, safety and antihyperlipidemic potential. Sci Rep. 2019 Nov 19;9(1):16105. doi: 10.1038/s41598-019-52645-0, PMID 31695118.
7. Faraji E, Mohammadi M, Mahboobian MM. Development of the binary and ternary atorvastatin solid dispersions: *in vitro* and *in vivo* investigations. BioMed Res Int. 2021 Sep 6;2021:6644630. doi: 10.1155/2021/6644630, PMID 34527740.
8. Apeji YE, Oyi AR, Isah AB, Allagh TS, Modi SR, Bansal AK. Development and optimization of a starch-based co-processed excipient for direct compression using mixture design. AAPS PharmSciTech. 2018 Feb;19(2):866-80. doi: 10.1208/s12249-017-0887-x, PMID 29038987.
9. Saha S, Shahiwala AF. Multifunctional co-processed excipients for improved tabletting performance. Expert Opin Drug Deliv. 2009 Feb;2(6):197-208.
10. Karavas E, Georgarakis E, Sigalas MP, Avgoustakis K, Bikiaris D. Investigation of the release mechanism of a sparingly water-soluble drug from solid dispersions in hydrophilic carriers based on physical state of drug, particle size distribution and drug-polymer interactions. Eur J Pharm Biopharm. 2007;66(3):334-47. doi: 10.1016/j.ejpb.2006.11.020. PMID 17267194.
11. Bikiaris D, Papageorgiou GZ, Stergiou A, Pavlidou E, Karavas E, Kanaze F. Physicochemical studies on solid dispersions of poorly water-soluble drugs: evaluation of capabilities and limitations of thermal analysis techniques. Thermochim Acta. 2005:58-67. doi: 10.1016/j.tca.2005.09.011.
12. Al-Hamidi H, Edwards AA, Mohammad MA, Nokhodchi A. To enhance dissolution rate of poorly water-soluble drugs: glucosamine hydrochloride as a potential carrier in solid dispersion formulations. Colloids Surf B Biointerfaces. 2010;76(1):170-8. doi: 10.1016/j.colsurfb.2009.10.030. PMID 19945828.
13. Surini S, Evangelista CN, Iswandana R. Development of glimepiride solid dispersion using the coprocessed excipients of polyvinylpyrrolidone, maltodextrin, and polyethylene glycol. J Young Pharm. 2018 Jul;10(2s):S45-50. doi: 10.5530/jyp.2018.2s.9.
14. Chiou WL, Riegelman S. Preparation and dissolution characteristics of several fast-release solid dispersions of griseofulvin. J Pharm Sci. 1969 Dec;58(12):1505-10. doi: 10.1002/jps.2600581218, PMID 5353269.
15. Adibkia K, Javadzadeh Y, Dastmalchi S, Mohammadi G, Niri FK, Alaei Beirami M. Naproxen-eudragit RS100 nanoparticles: preparation and physicochemical characterization. Colloids Surf B Biointerfaces. 2011 Nov 18;83(1):155-9. doi: 10.1016/j, PMID 21130612.
16. Barzegar Jalali M, Alaei Beirami M, Javadzadeh Y, Mohammadi G, Hamidi A, Andalib S. Comparison of physicochemical characteristics and drug release of diclofenac sodium-eudragit®. Powder Technol; RS100 Nanoparticles and Solid Dispersions. 2012 Mar;219:211–6. doi: 10.1016/j.powtec.2011.12.046.
17. Chaheen M, Sanchez Ballester NM, Bataille B, Yassine A, Belamie E, Sharkawi T. Development of coprocessed chitin-calcium carbonate as multifunctional tablet excipient for direct compression. J Pharm Sci. 2018 Aug;107(8):2152-9. doi: 10.1016/j.xphs.2018.04.013, PMID 29698724.
18. Kaur L, Kaur T, Singh A, Singh A. Formulation development and solubility enhancement of rosuvastatin calcium by using hydrophilic polymers and solid dispersion method. Int J Curr Pharm. 2021;13(6):50-5.
19. Sahu VK, Sharma N, Sahu PK, Saraf SA. Formulation and evaluation of floating-mucoadhesive microspheres of novel natural polysaccharide for site specific delivery of ranitidine hydrochloride. Int J App Pharm. 2017;9(3):15-9. doi: 10.22159/ijap.2017v9i3.16137.
20. Deshmukh MT, Mohite SK. Formulation and characterization of olanzepineloaded mucoadhesive microspheres. Asian J Pharm Clin Res 2017;10(4). doi: 10.22159/ajpcr.2017.v10i4.16659.
21. Velmurugan S, Ashraf MA. Preparation and evaluation of maravirocmucoadhesive microspheres for gastro retentive drug delivery. Int J Pharm Pharm Sci. 2015;7(5):208-14.
22. El-Assal MI, Samuel D. Optimization of rivastigmine chitosan nanoparticles for neurodegenerative Alzheimer; *in vitro* and ex vivo characterizations. Int J Pharm Pharm Sci. 2022;14(1):17-27. doi: 10.22159/ijpps.2022v14i1.43145.
23. Lal K, Purohit A, Ram H. Glucose homeostatic and pancreas protective potential of tecomella undulata root extract in streptozotocin induced diabetic rats. Asian J Pharm Clin Res 2017;10(6). doi: 10.22159/ajpcr.2017.v10i6.17997.
24. Dhore PW, Dave VS, Saoji SD, Bobde YS, Mack C, Raut NA. Enhancement of the aqueous solubility and permeability of a poorly water soluble drug ritonavir via lyophilized milk-based solid dispersions. Pharm Dev Technol. 2017;22(1):90-102. doi: 10.1080/10837450.2016.1193193, PMID 27291246.
25. Dhore PW, Dave VS, Saoji SD, Gupta D, Raut NA. Influence of carrier (Polymer) type and drug-carrier ratio in the development of amorphous dispersions for solubility and permeability enhancement of ritonavir. J Excipients Food Chem. 2017;8(3):75-92.
26. Dixit P, Jain DK, Dumbwani J. Standardization of an ex vivo method for determination of intestinal permeability of drugs using everted rat intestine apparatus. J Pharmacol Toxicol Methods. 2012 Jan;65(1):13-7. doi: 10.1016/j.vascn.2011.11.001. PMID 22107724.
27. Kim JS, Kim MS, Park HJ, Jin SJ, Lee S, Hwang SJ. Physicochemical properties and oral bioavailability of amorphous atorvastatin hemi-calcium using spray-drying and SAS process. Int J Pharm. 2008 Jul;359(1-2):211-9. doi: 10.1016/j.ijpharm.2008.04.006. PMID 18501538.
28. Choudhary A, Rana AC, Aggarwal G, Kumar V, Zakir F. Development and characterization of an atorvastatin solid dispersion formulation using skimmed milk for improved oral bioavailability. Acta Pharmaceutica Sinica B. 2012;2(4):421-8. doi: 10.1016/j.apsb.2012.05.002.
29. Iqbal R, Qureshi OS, Yousaf AM, Raza SA, Sarwar HS, Shahnaz G. Enhanced solubility and biopharmaceutical performance of atorvastatin and metformin via electrospun polyvinylpyrrolidone-hyaluronic acid composite nanoparticles.

Eur J Pharm Sci. 2021 Jun 1;161:105817. doi: 10.1016/j.ejps.2021.105817. PMID 33757829.

30. Kamran M, Khan MA, Shafique M, Rehman Mu, Ahmed W, Abdullah. Development and characterization of binary solid lipid nano suspension of atorvastatin: *in vitro* drug release and *in vivo* pharmacokinetic studies. Nanosci Nanotechnol. 2019 Nov;11(11):1522-30. doi: 10.1166/nnl.2019.3039.
31. Balcerowiak W. Comments on pentaerythritol DSC. J Therm Anal. 1996 Jun;46(6):1881-3. doi: 10.1007/BF01980791.
32. Alshaya HA, Alfahad AJ, Alsulaihem FM, Aodah AH, Alshehri AA, Almughem FA. Fast-dissolving nifedipine and atorvastatin calcium electrospun nanofibers as a potential buccal delivery system. Pharmaceutics. 2022 Feb 4;14(2):358. doi: 10.3390/pharmaceutics14020358, PMID 35214093.
33. Golderg AH, Gibaldi M, Kanig JL, Mayersohn M. Increasing dissolution rates and gastrointestinal absorption of drugs via solid solutions and eutectic mixtures IV. J Pharm Innov. 1995:307-14.
34. Goldberg AH, Gibaldi M, Kanig JL. Increasing dissolution rates and gastrointestinal absorption of drugs via solid solutions and eutectic mixtures III. J Pharm Sci. 1966 May;55(5):487-92. doi: 10.1002/jps.2600550508.